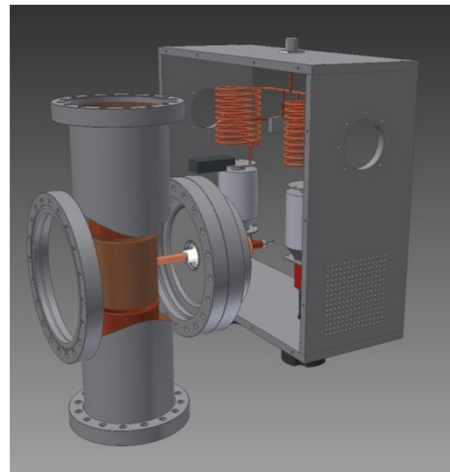


THE NEW AXIAL BUNCHER AT INFN-LNS

Antonio Caruso
INFN-LNS



Talking points

- **Main reasons for a new axial buncher**
- **Buncher study**
- **Design: mechanical, electrical, numerical simulations**
- **LLRF system of the buncher**
- **Test and measurements**
- **Conclusions**
- **References**
- **Discussion**

New axial buncher, main reasons.

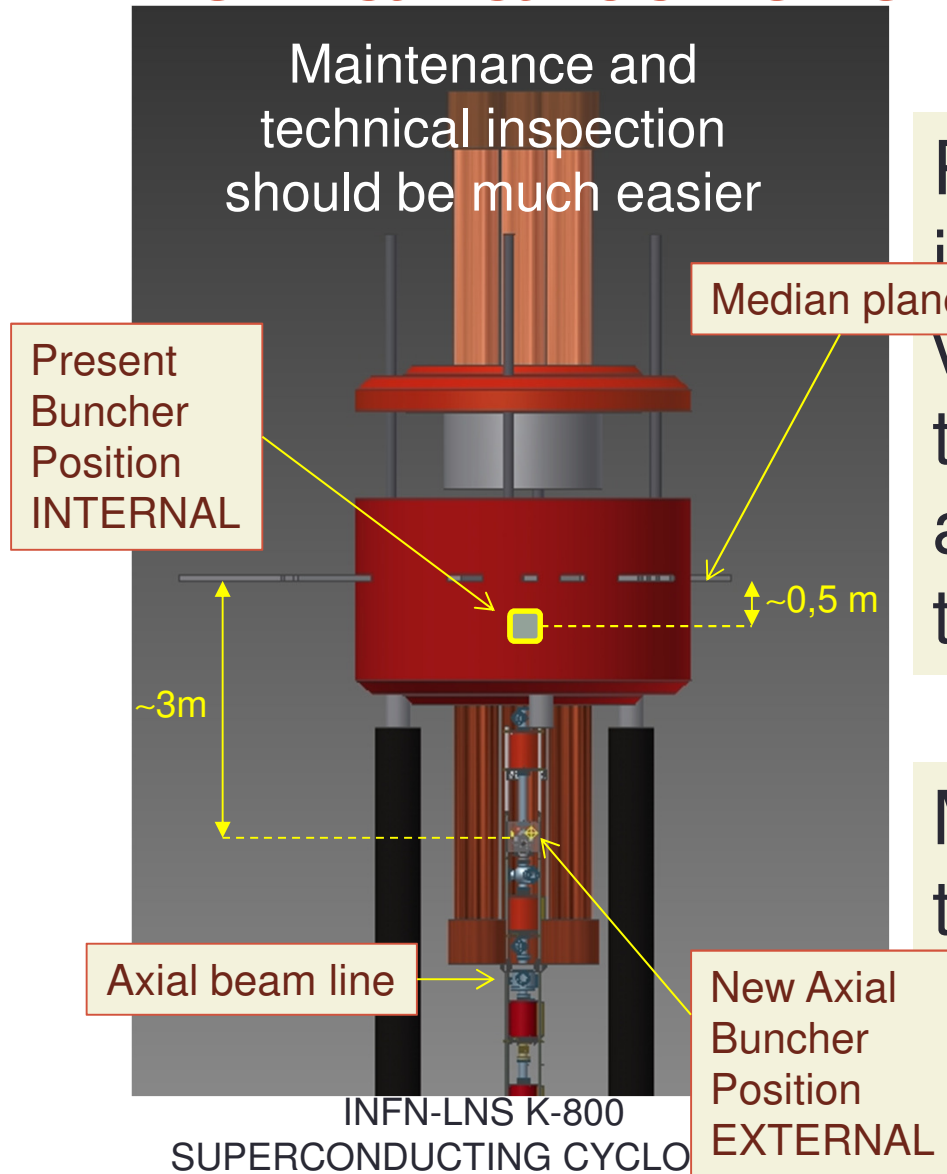


INFN-LNS K-800
SUPERCONDUCTING CYCLOTRON

Present axial buncher is installed along the vertical beam line inside the yoke of the cyclotron at about half meter from the median plane.

Maintenance and technical inspection are very difficult to carry out in this situation.

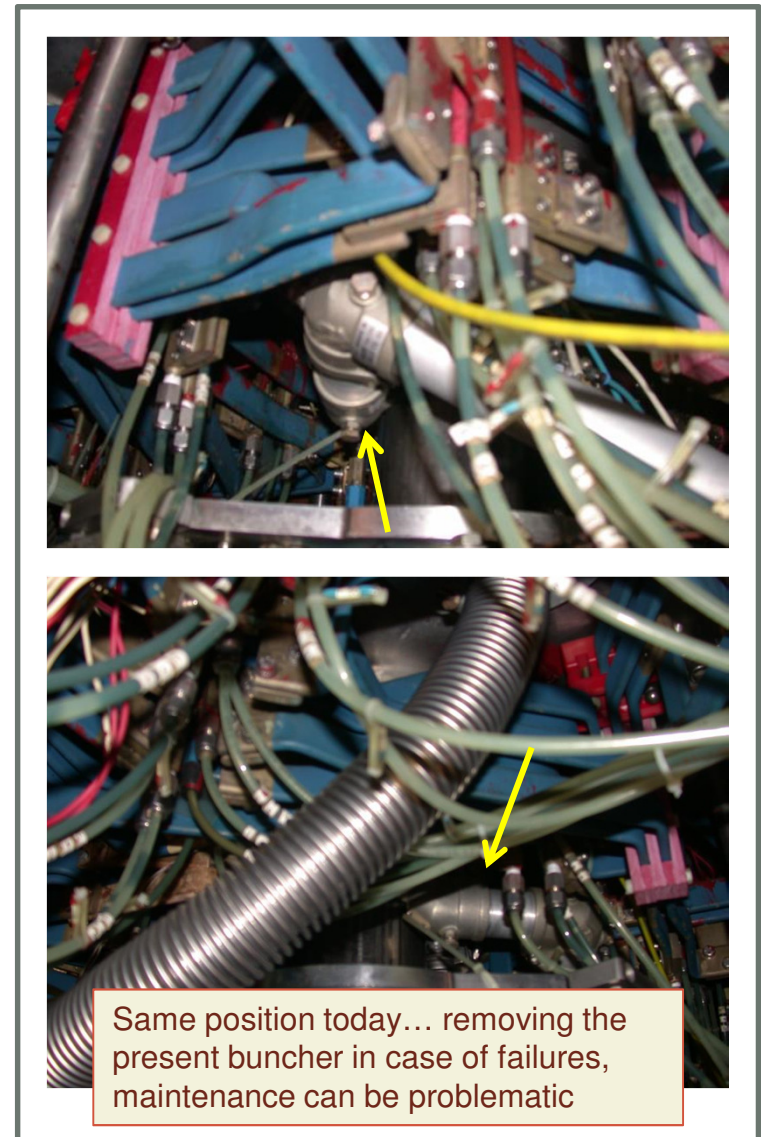
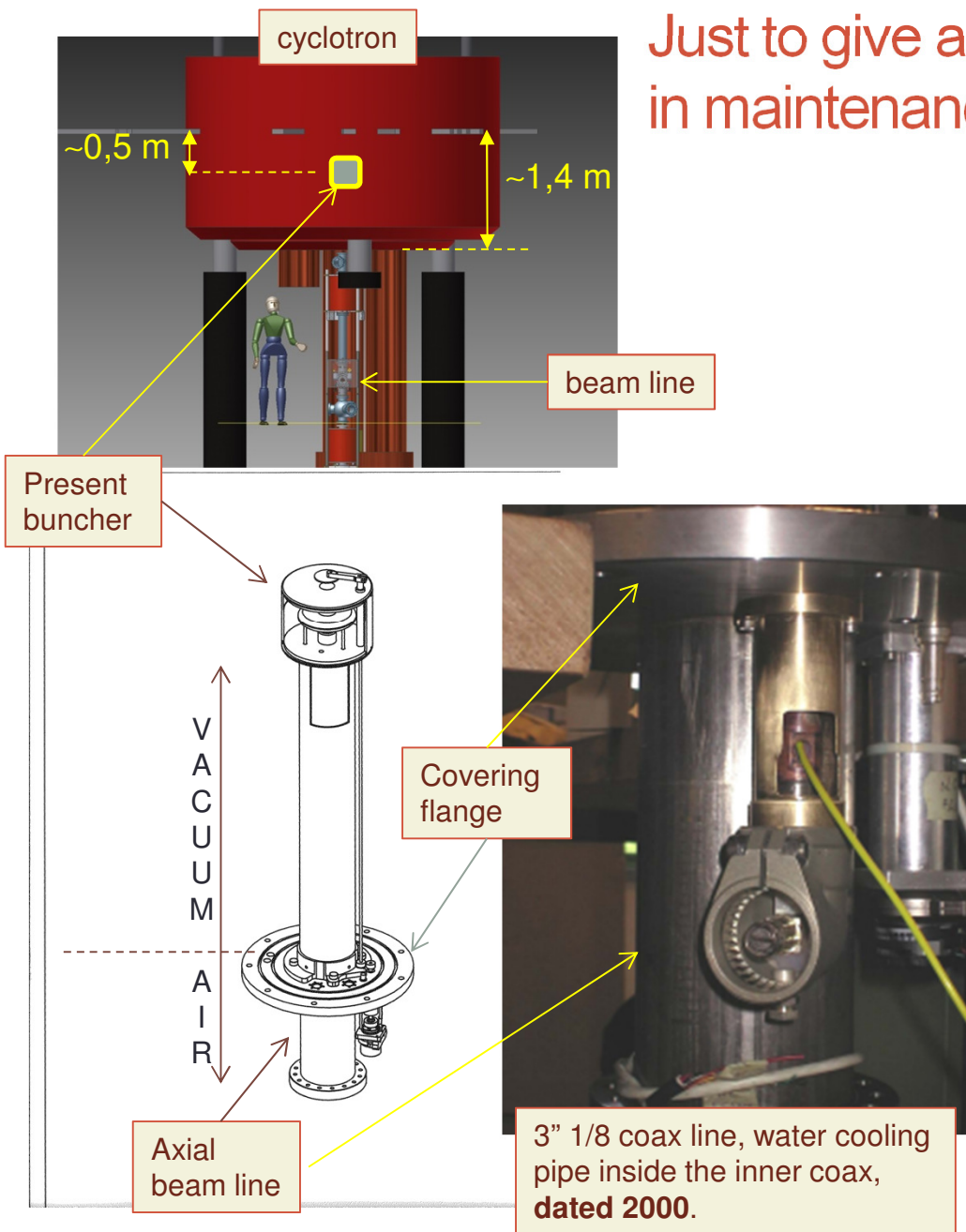
New axial buncher, main reasons.

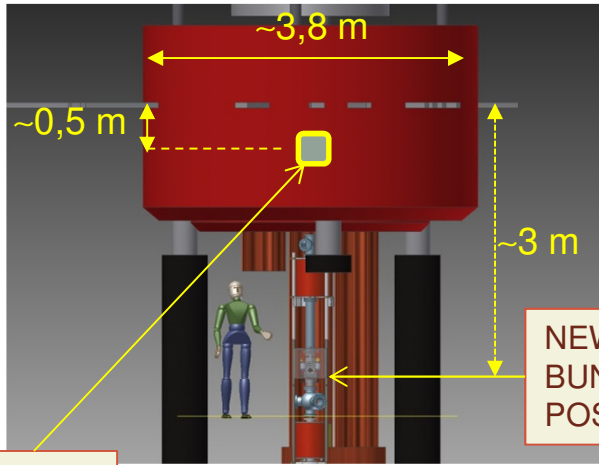


Present axial buncher is installed along the vertical beam line inside the yoke of the cyclotron at about half meter from the median plane.

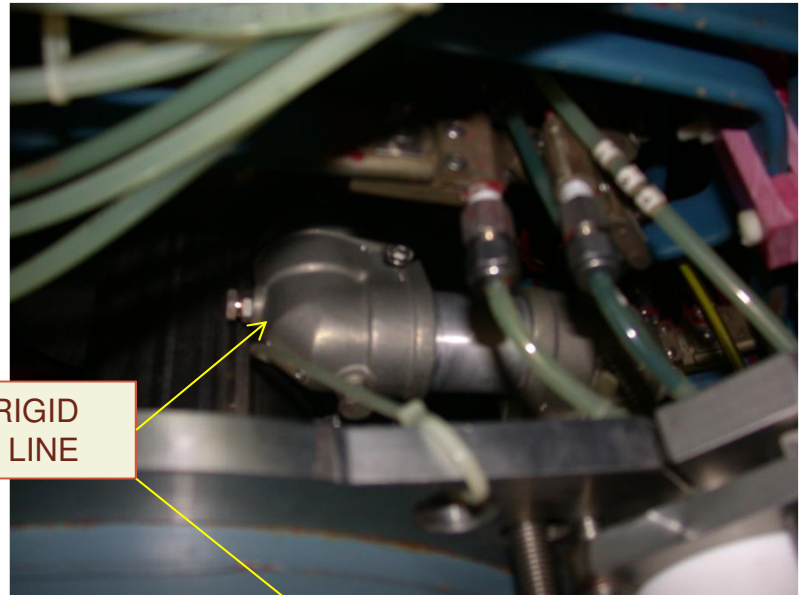
Maintenance and technical inspection are very difficult to carry out in this situation.

Just to give an idea of the complexity involved in maintenance work of the present buncher



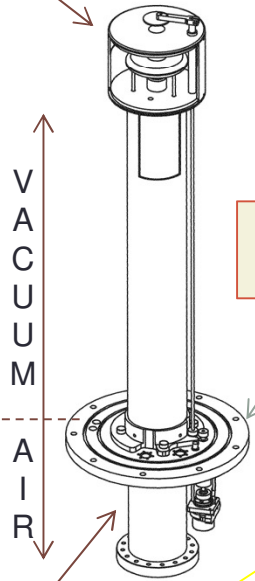


NEW AXIAL BUNCHER POSITION

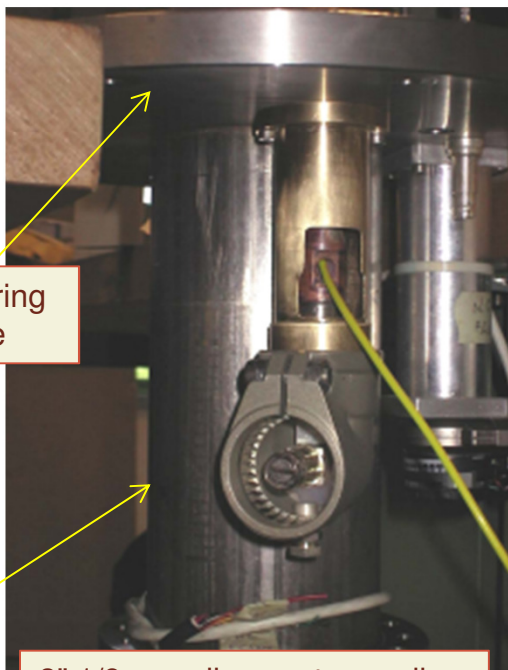


3" 1/8 RIGID COAX LINE

Present buncher



Axial beam line



Covering flange

3" 1/8 coax line, water cooling pipe inside the inner coax, in 2000.



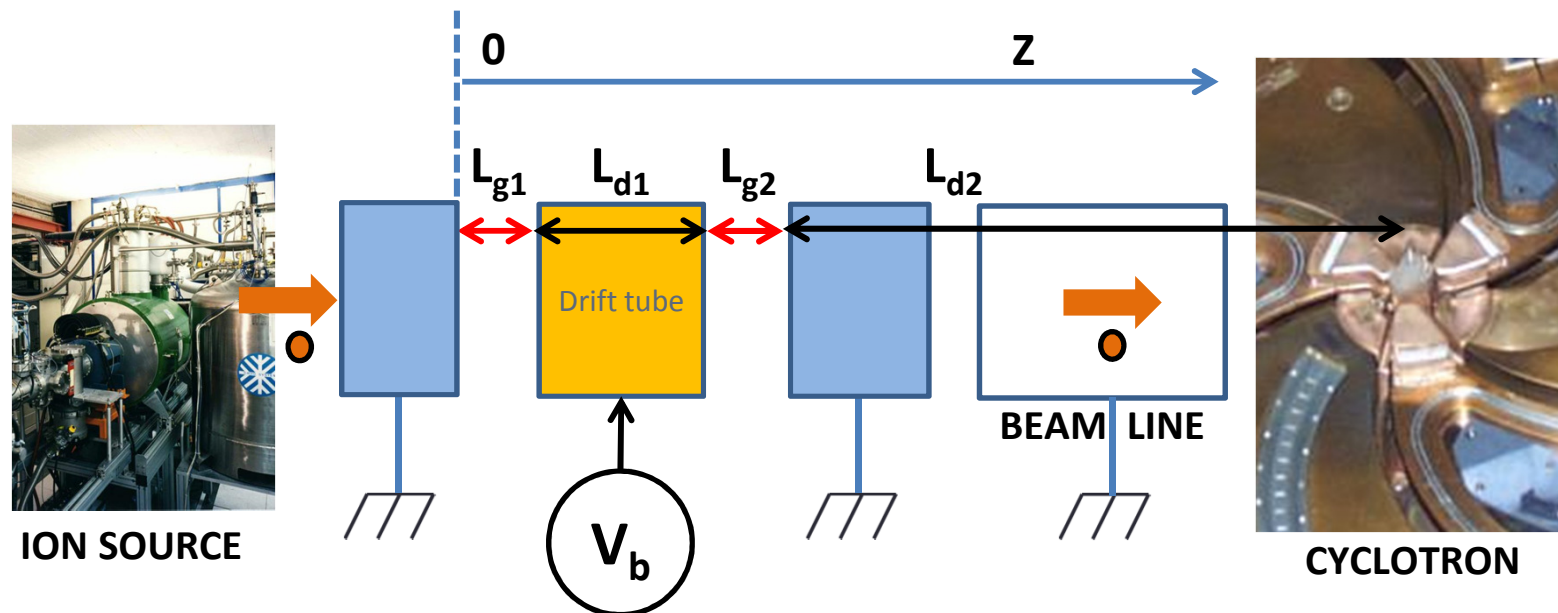
Axial Beam line

Same position today...

THE AXIAL BUNCHER STUDY

the buncher consists of a drift tube driven by a sinusoidal RF signal in the range of 15-50 MHz, a matching box, an amplifier, and an electronic control system.

Basic two gap buncher structure



$$V_B = V_{MB} \sin(\omega t + \varphi_0)$$

It is a **drift tube**, fed by a sinusoidal voltage and placed between two grounded tube electrodes.

L_{g1} and L_{g2}

are the two gaps of 5 mm length

The distance between the Buncher and the inflector at the cyclotron central region (time focus) is 3011 mm, and it is imposed by mechanical constraints

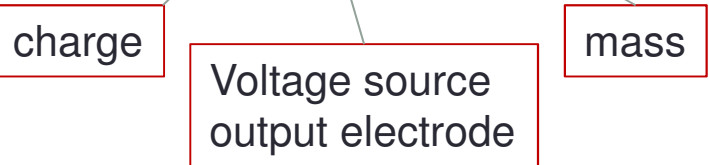
Ion source beam table

0	1	2	3	4
"Ion"	"MeV/n"	"Vo(kV)"	Fh2(MHz)"	"Vb(Volt)"
"4 He 1+"	25	17	25.576	80.369
"4 He 2+"	62	20.22	39.312	86.762
"4 He 2+"	80	24.72	43.617	105.709
"9 Be 3+"	45	22.21	33.742	95.018
"12 C 3+"	23	15.47	24.41	66.123
"13 C 4+"			42	102.74
"27Al 9+"			71	84.484
"40Ar9+"			2.9	64.61
"48Ca9+"			35	39.529
"48Ca15+"			42	100.966
"58Ni 21+"	50	22.52	35.457	96.22
"84Kr 17+"	20	16.81	22.9	71.831
12Sn 31+"	43	25.65	33.08	109.611
16Sn 21+"	17	16.03	21.15	68.5
29Xe 31+"	35	24.03	29.835	102.685
97 Au 31+"	15	16.62	20.071	71.047
197 Au 36"	23	21.17	24.41	90.5



We now illustrate the typical case for α particles

$$v_{z0} = \sqrt{2q_i V_s / m_i} \quad \text{particle velocity } z=0$$

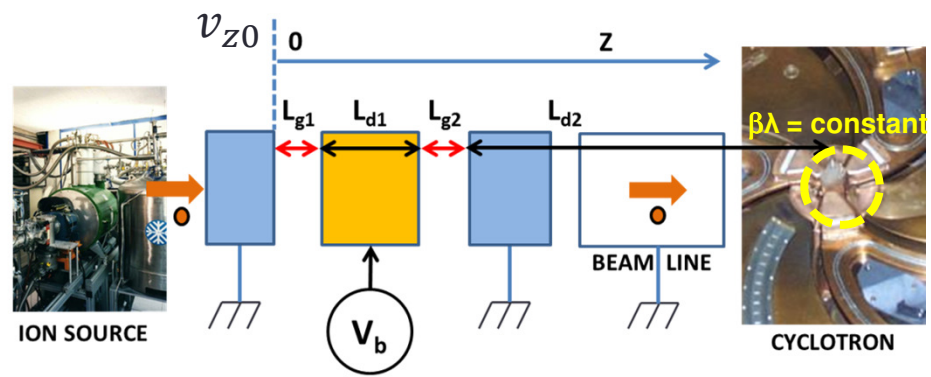


(with f cyclotron frequency) is the path of the particles in one period and, because of the fixed geometry of the cyclotron central region, has to be constant

$$\beta\lambda = v_{z0} / f$$

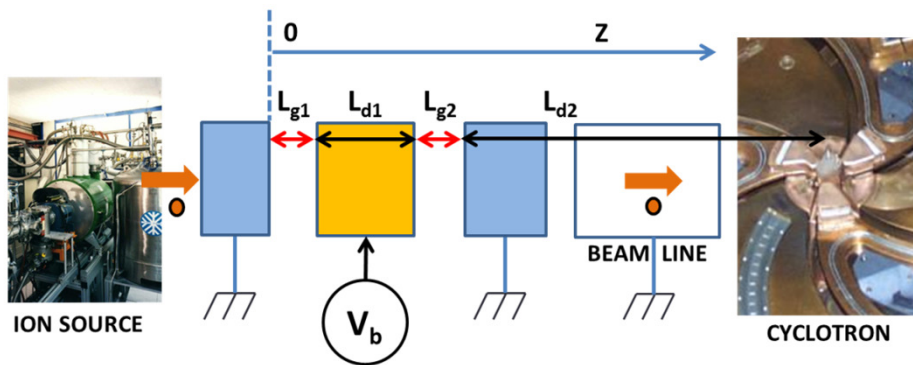
$L_{d1} = 83.5 \text{ mm}$ drift tube length

This length is chosen so that $L_{d1} + L_{g1}$ is an odd integer multiple of the $(N+1/2)\beta\lambda/2$ in our case with $N=2$ and $\beta\lambda=35,4 \text{ mm}$



α Charged particle case

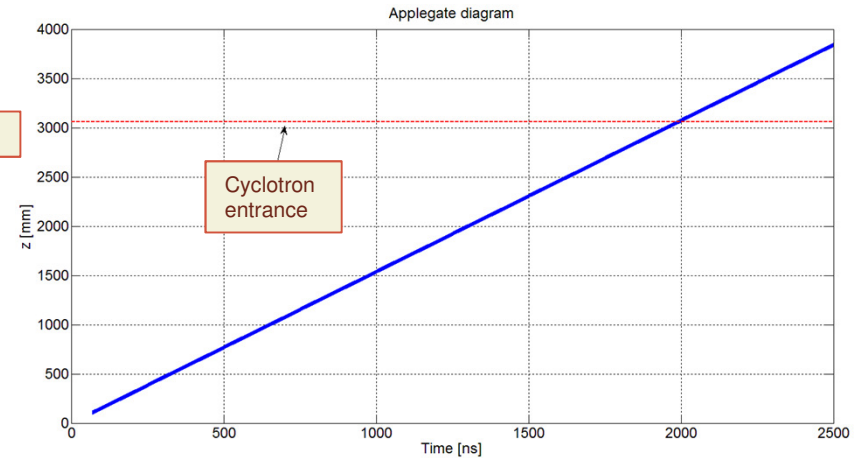
0	1	2	3
"Ion"	"MeV/n"	"Vo(kV)"	Fh2(MHz)"
"4 He 1+"	25	17	25.576
"4 He 2+"	62	20.22	39.312
"4 He 2+"	80	24.72	43.617



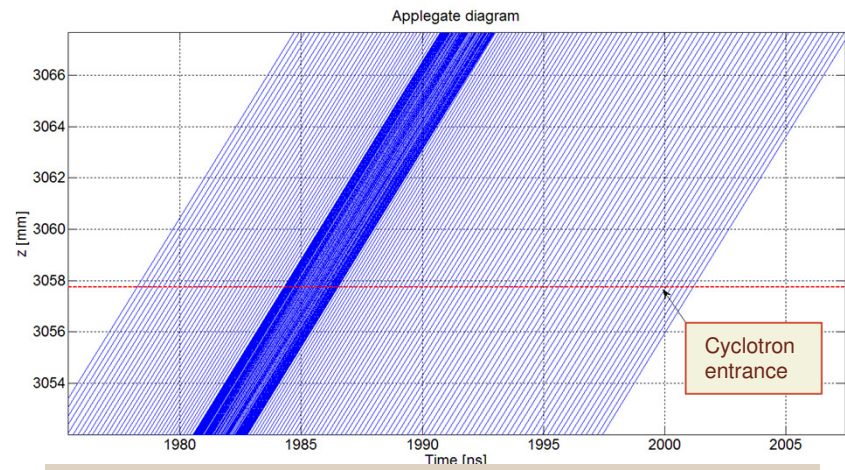
- $L_{g1} = L_{g2} = 5 \text{ mm}$
- $L_{d1} = 83.5 \text{ mm}$
- $L_{d2} = 3011 \text{ mm} - L_{g2} - (L_{d1} / 2) = 2964.25 \text{ mm}$
- $v_{z0} = \sqrt{\frac{2 q_i V_s}{m_i}}$ particle velocity when it arrives at the $z = 0$ position, due to the ion source voltage

- Ion specie considered = ${}^4\text{He}^{2+}$
- Ion source voltage - $V_s = 24.72 \text{ kV}$
- $V_B = V_{MB} \sin(\omega t + \varphi_0)$
- $V_{MB} = 70.1174 / 0.95 \text{ V}$
- $\omega = 2\pi \cdot 43.617 \cdot 10^6 \text{ rad/s}$
- $\beta_0 \lambda_0 = \frac{v_{z0}}{f} = 35.28 \text{ mm}$
- Cyclotron acceptance interval phase = 35°

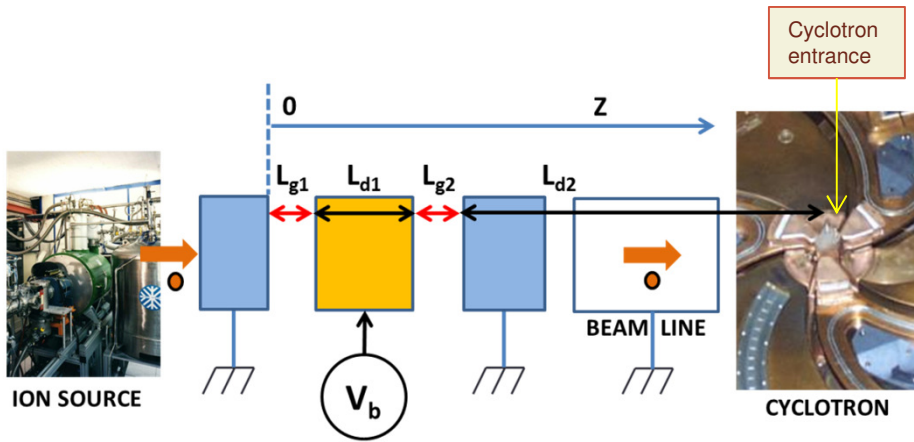
In this case the calculated particle trajectories are shown in the Applegate diagrams, referred to one period



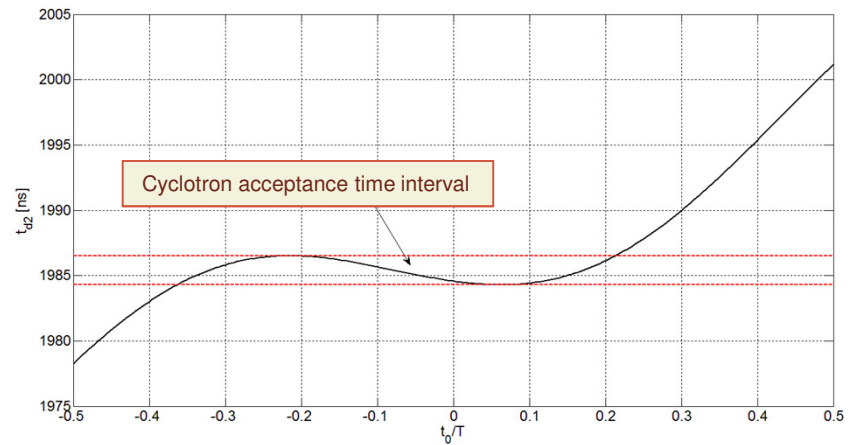
Applegate diagram. There is the indication of the z-position of the Cyclotron entrance.



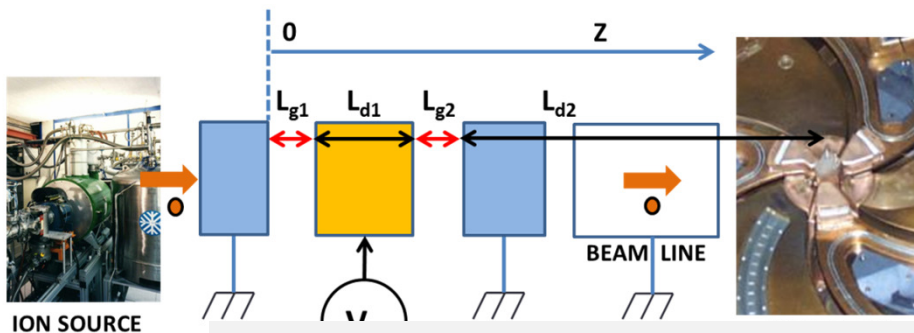
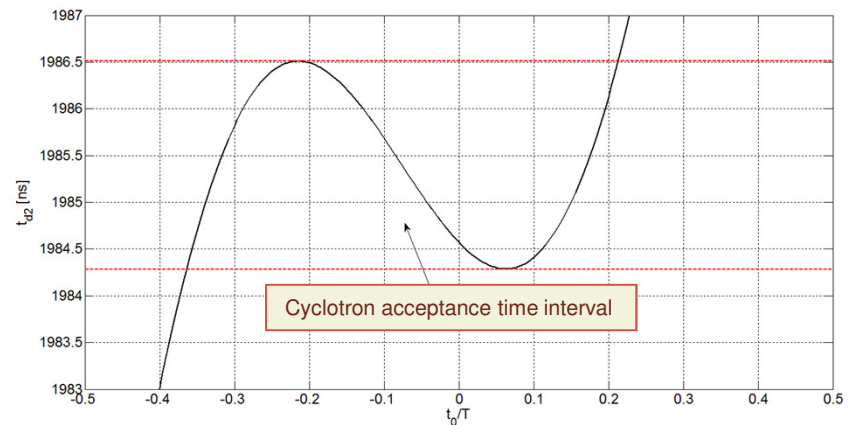
Enlarged view of the Applegate diagram. There is the indication of the z-position of the Cyclotron entrance.



In the graph the plot of t_{d2} versus t_0/T is shown. The V_{MB} voltage has been applied to optimize the particle transmission within the cyclotron acceptance time, referred to the 35° phase. This is clearly shown, where the curve is tangent to the dotted boundaries.



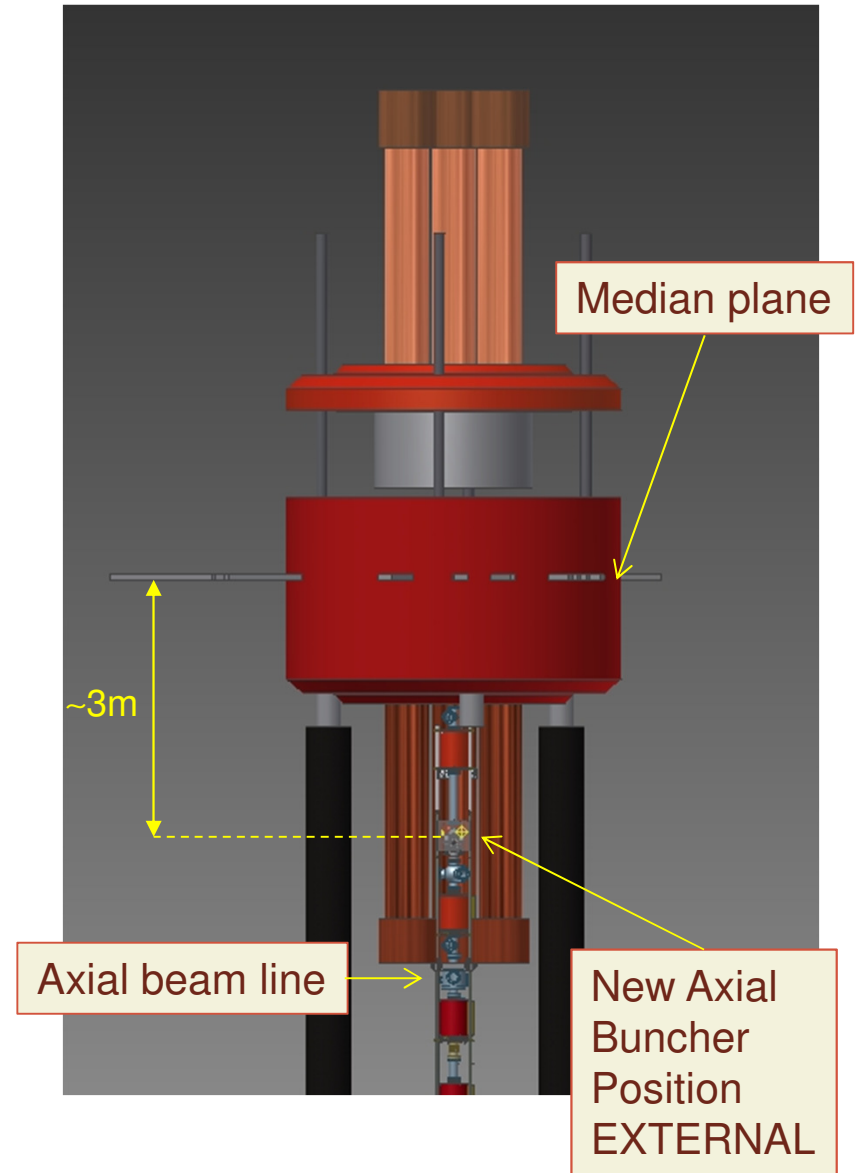
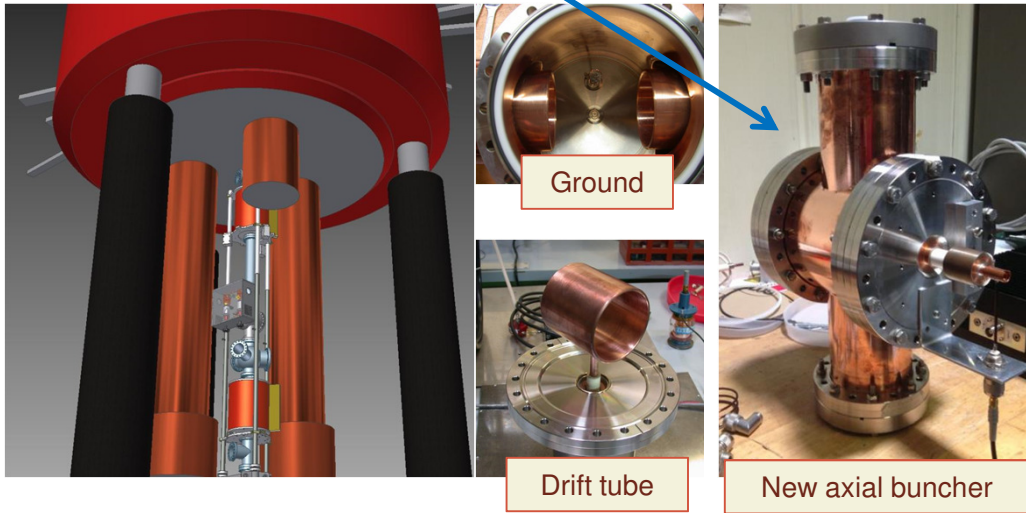
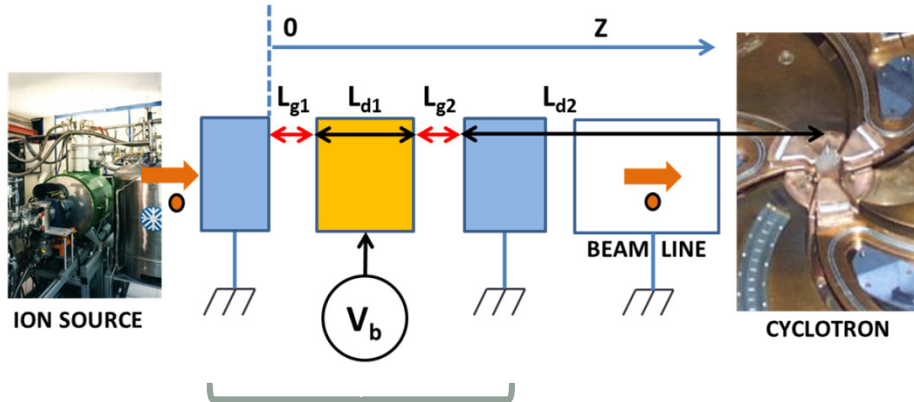
Arrival time of each particle at the Cyclotron entrance, with respect to the t_0 time when each particle arrives at the $z = 0$ position. $T = 1/f$.



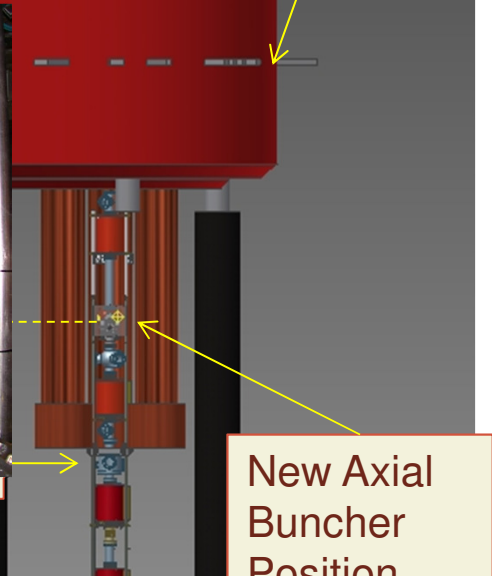
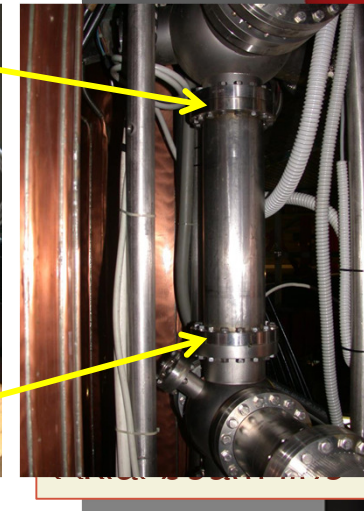
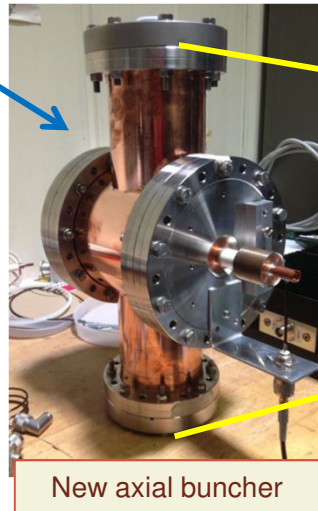
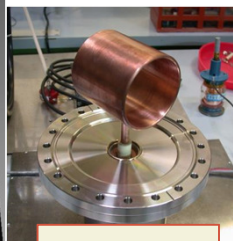
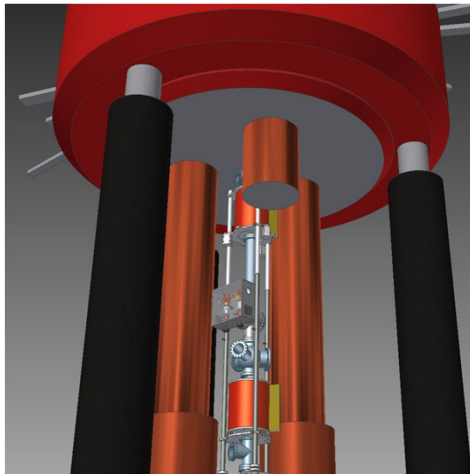
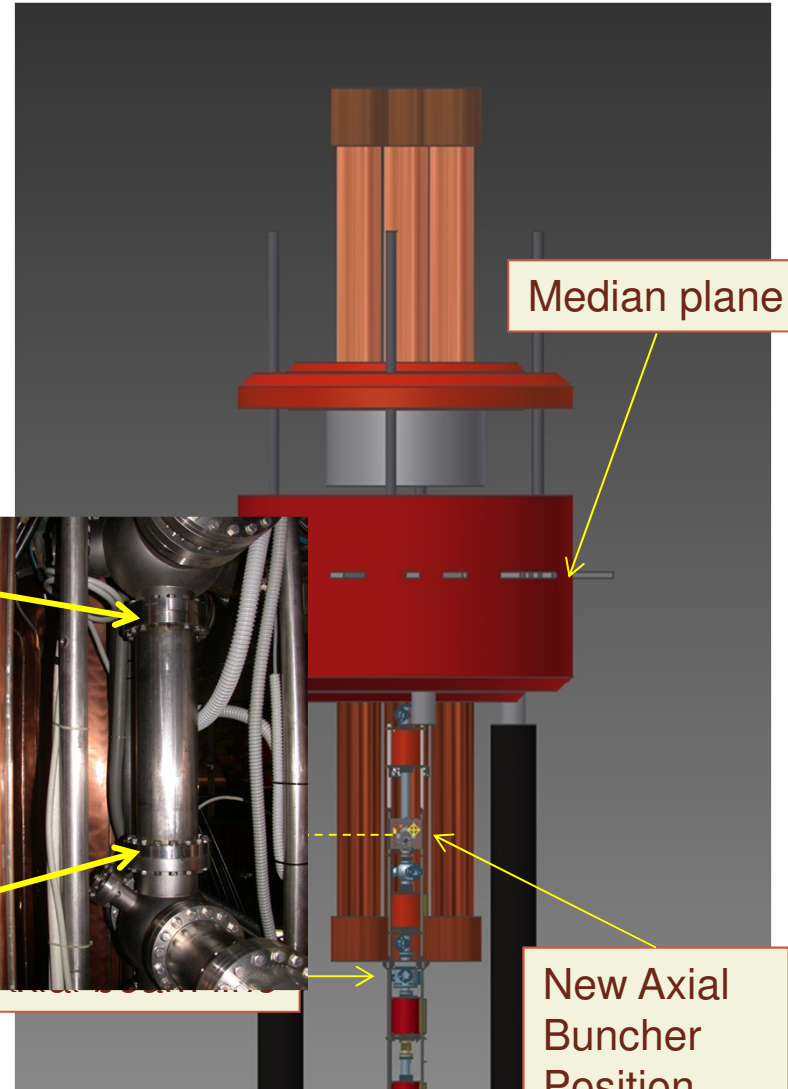
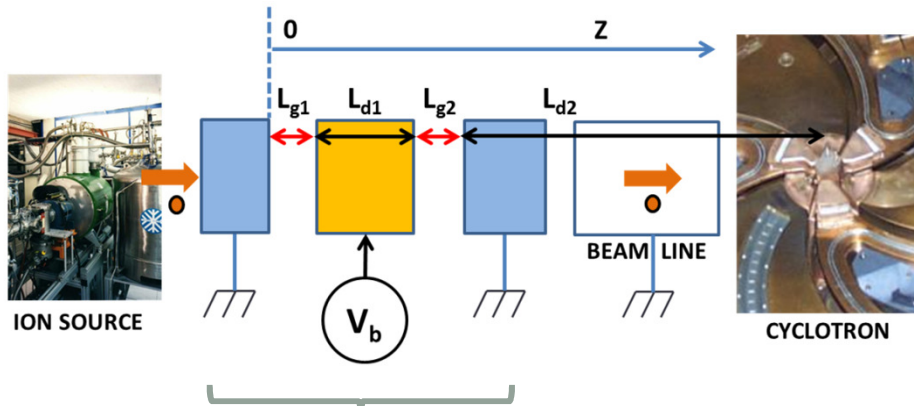
Under these conditions the particle transmission to the cyclotron is $TR = 57.6\%$, and the energy spread is $\Delta E/E = 1.15\%$.

$1/f$.

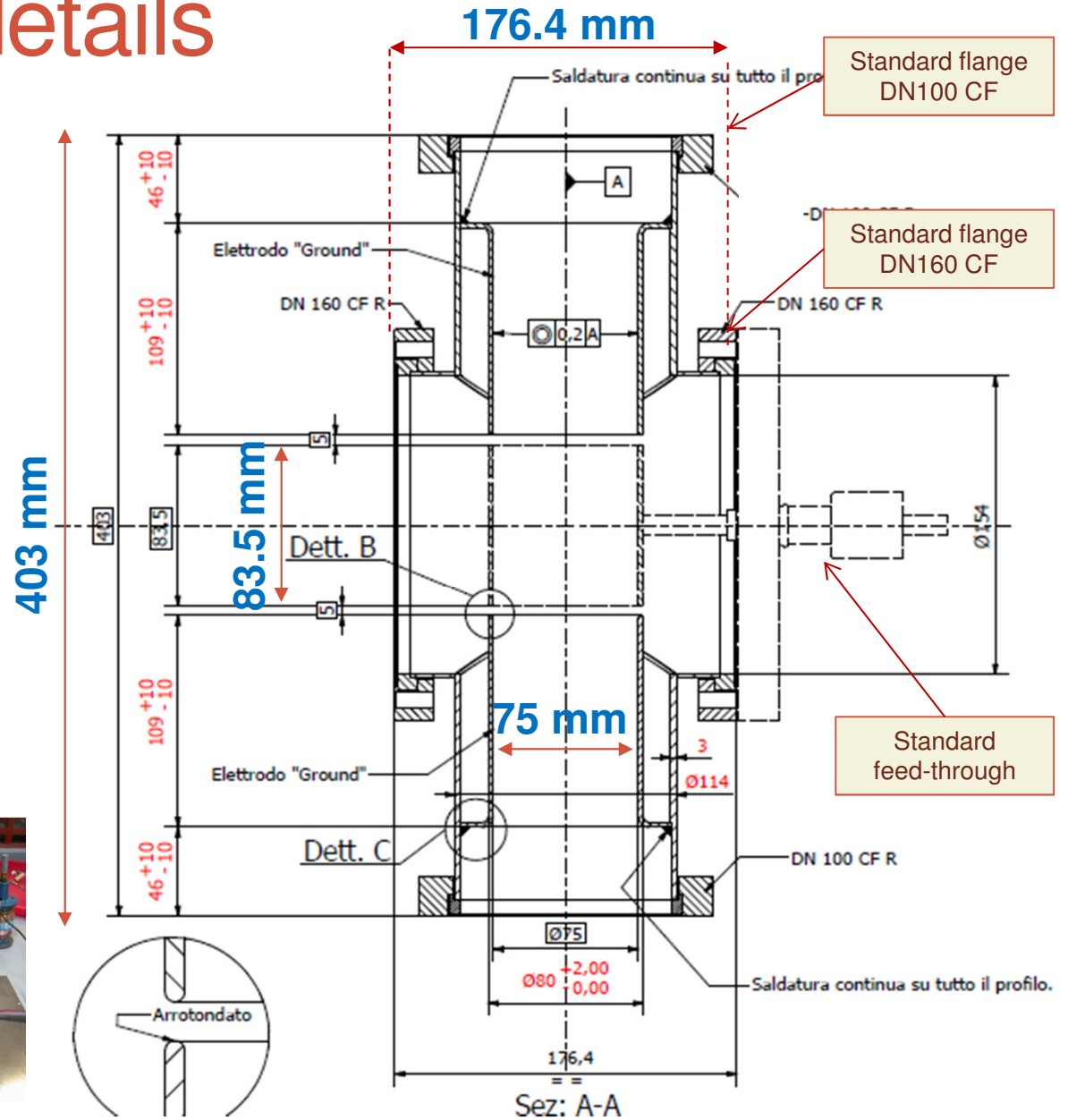
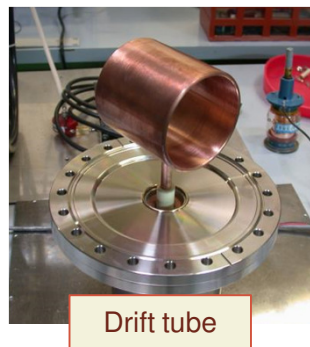
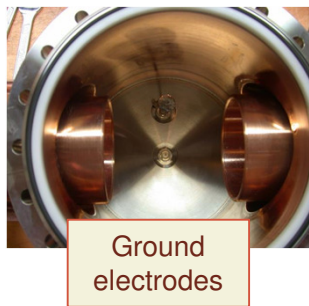
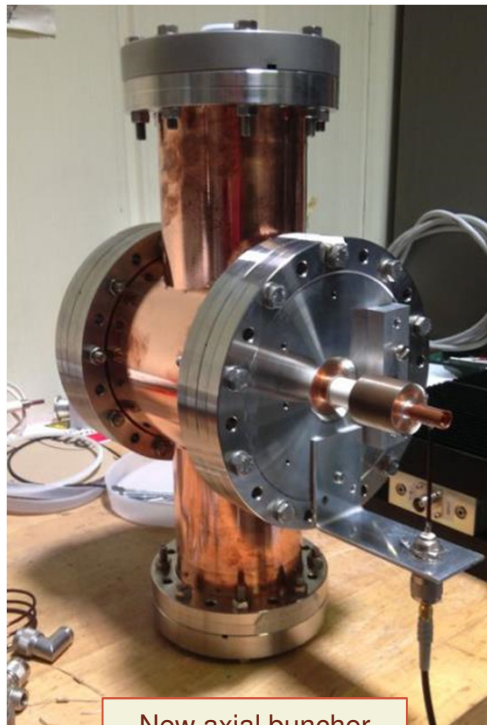
Mechanical design (drift tube mostly)



Mechanical design (drift tube mostly)



Mechanical details

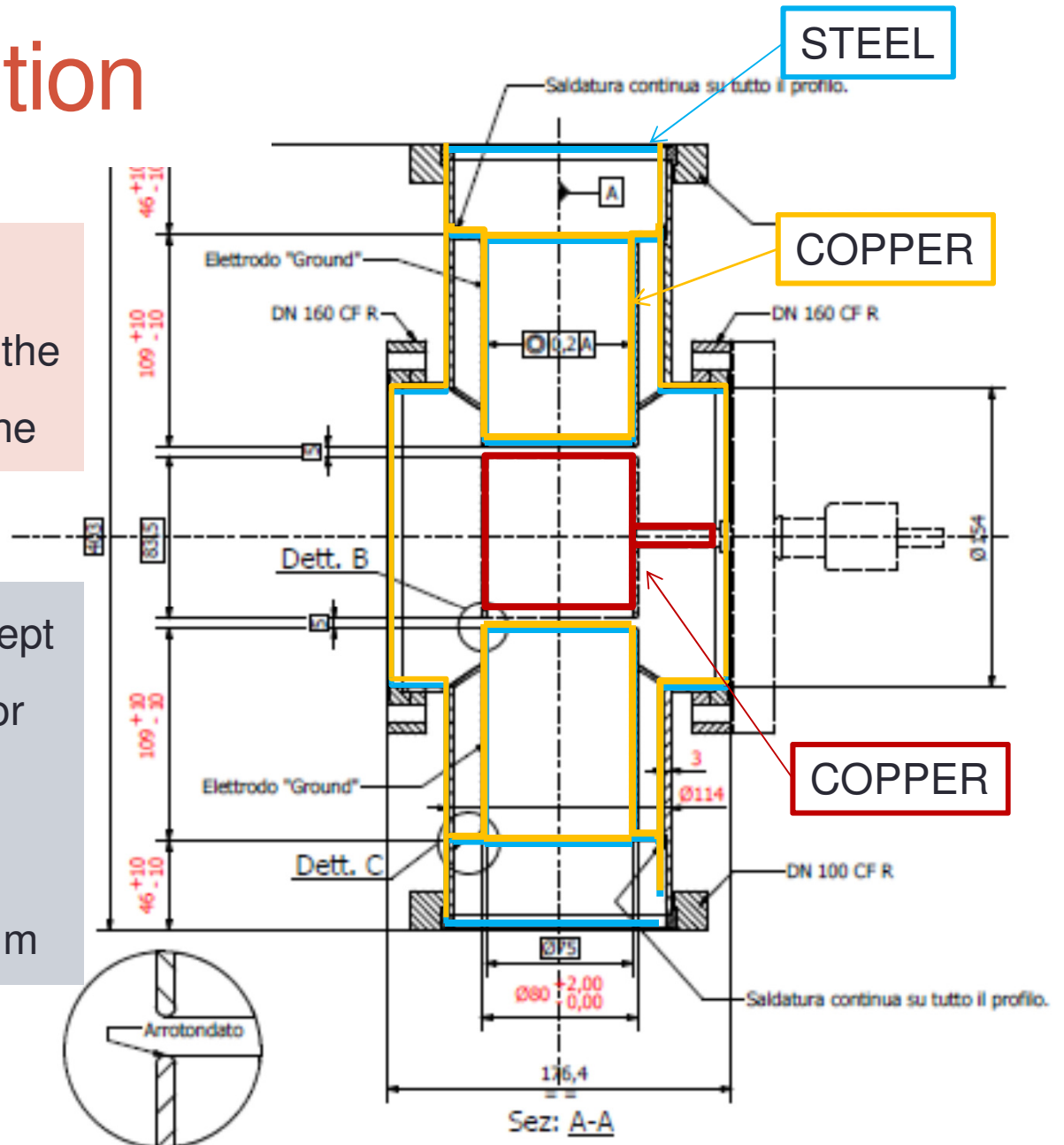


Copper deposition

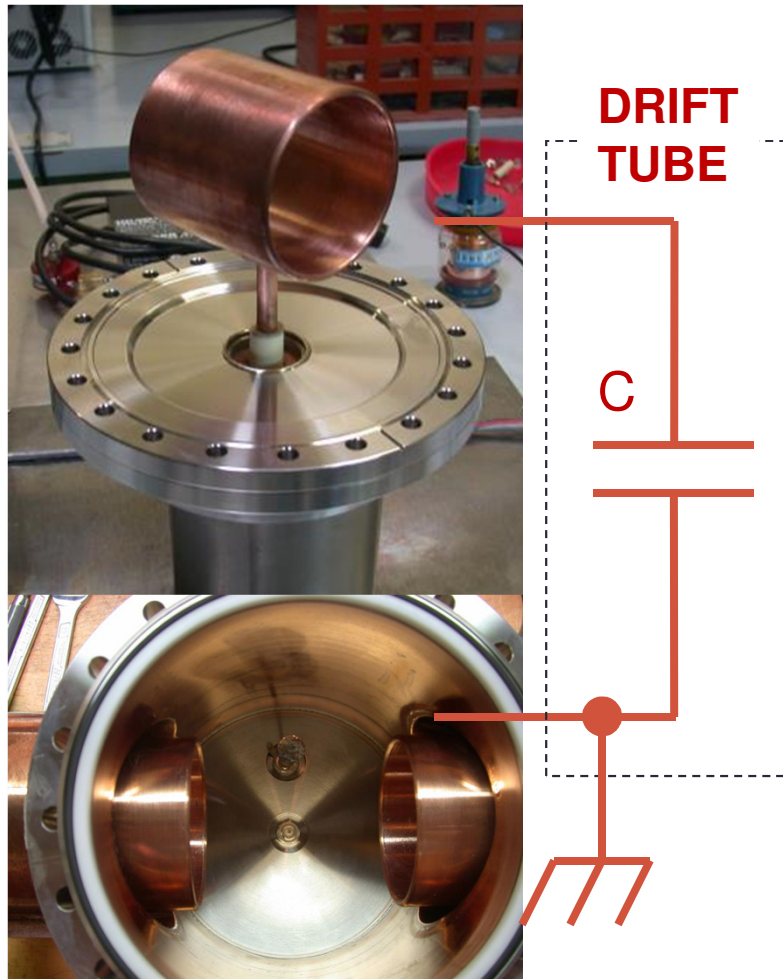
Drift tube copper made.
Galvanic copper deposition on the
ground electrodes and beam line



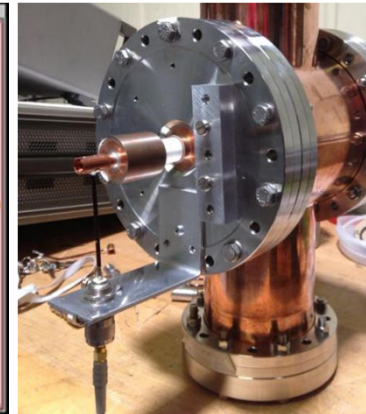
All surfaces are in copper (except
flanges). Consequently Q-factor
increases, prevents/minimizes
any copper surfaces facing a
steel surface under high vacuum



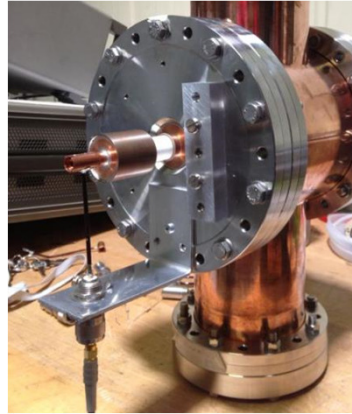
Electrical design



From the electrical point of view the **drift tube** can be seen as a **capacitance**.



An LCR meter confirms the simulated capacitance value of **about 27pF** and, with a vector network analyser, the **self-resonance of 352,75 MHz** has been measured through an **N-adaptor**.

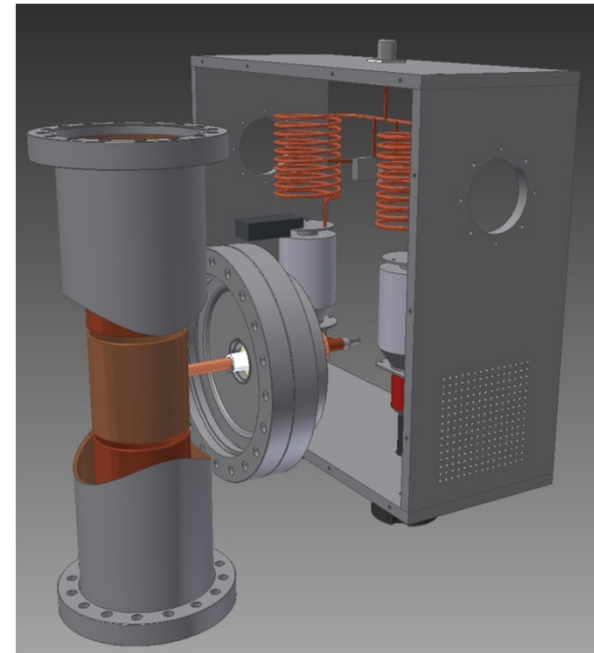
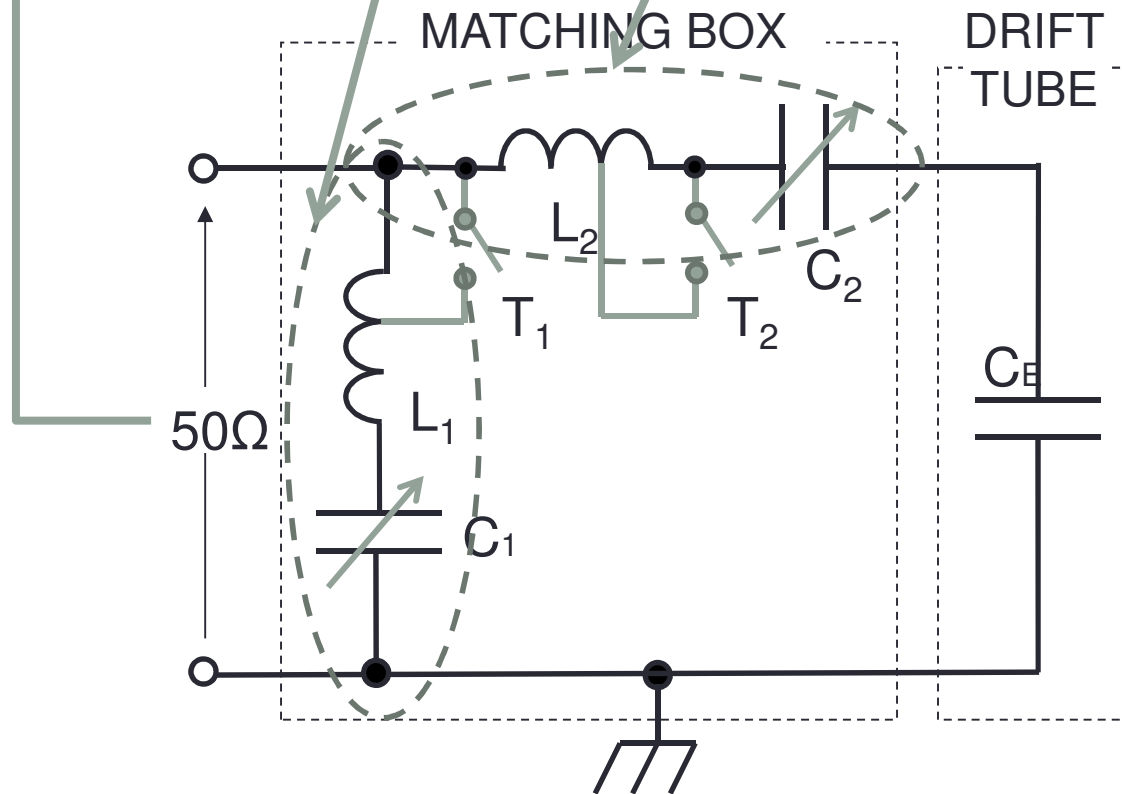
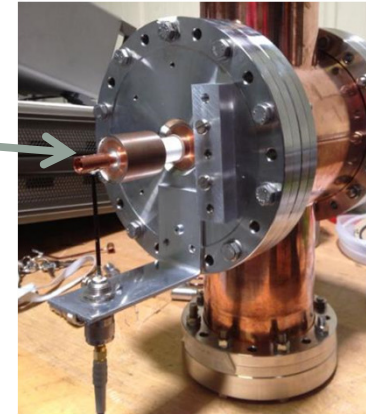


From a fixed frequency system
of 352.75 MHz
to the cyclotron frequency
bandwidth of 15-50 MHz

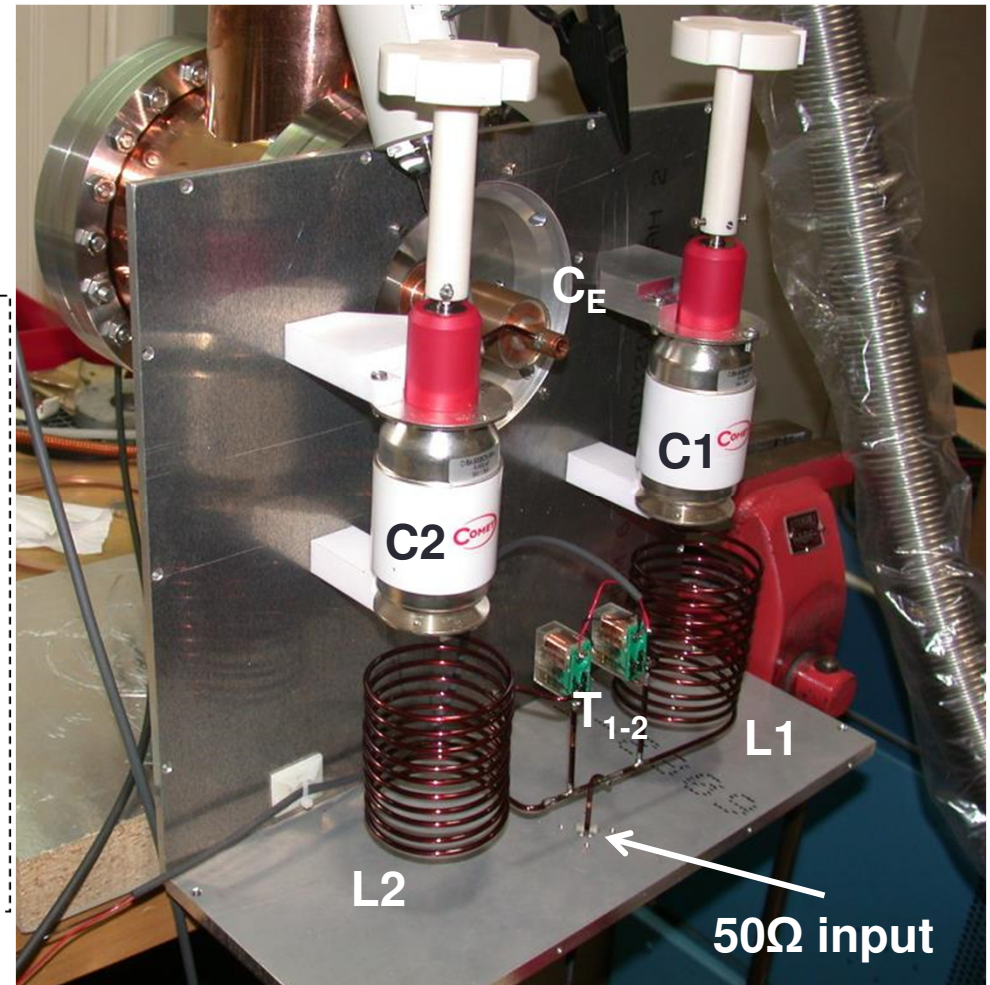
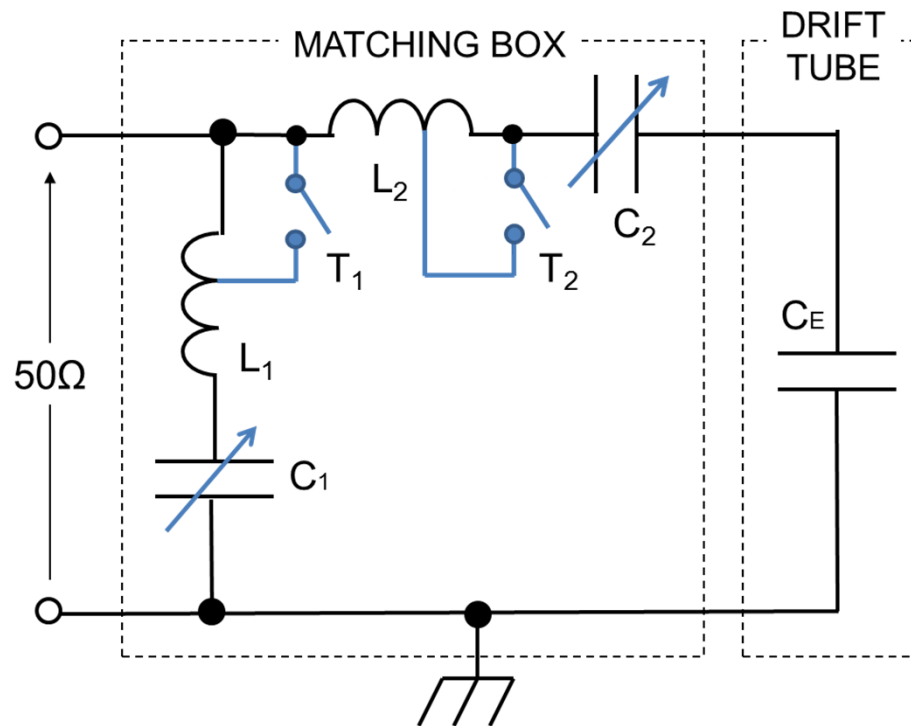
We need a sort of **transformer network** to match this
“drift tube capacitance” in terms of impedance
(standard 50 Ω) and total bandwidth (15-50 MHz)

Impedance transformer from Z_0 to buncher impedance Z_b

$$Z_{in} = \frac{Z_{shunt} \cdot (Z_{series} + Z_b)}{Z_{shunt} + (Z_{series} + Z_b)}$$

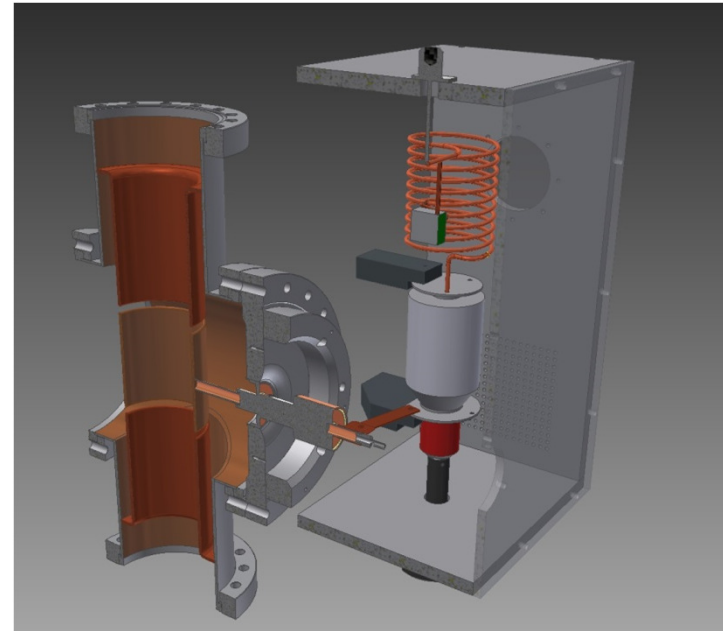
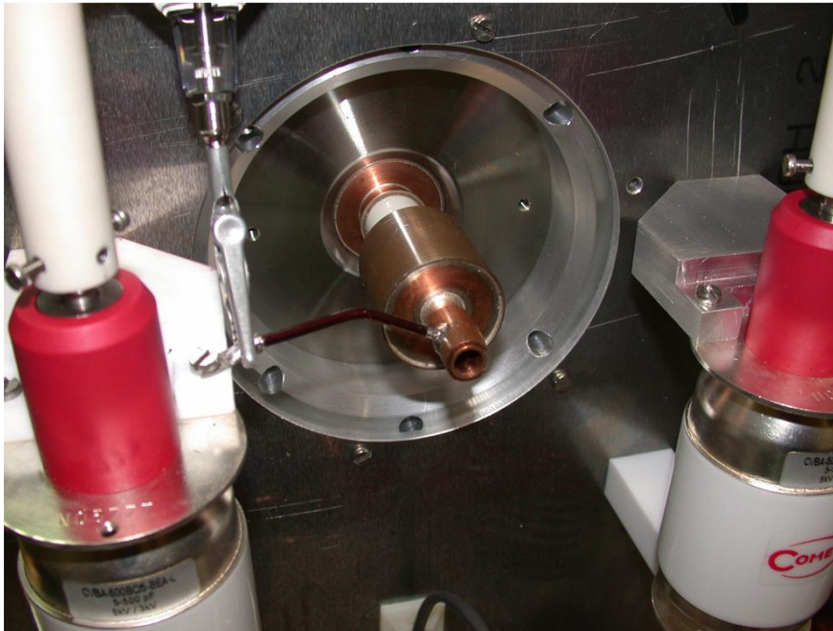


2 bandwidths to cover all the frequency range between 15 – 50 MHz



Lower Bandwidth: 13.3-25 MHz $L_1 = L_2 = 4.2 \mu\text{H}$ (T_1 - T_2 open)
Higher Bandwidth: 25-51 MHz $L_1 = L_2 = 1.3 \mu\text{H}$ (T_1 - T_2 closed)
 $C_1 = C_2$ variable capacitors between 5 – 500 pF

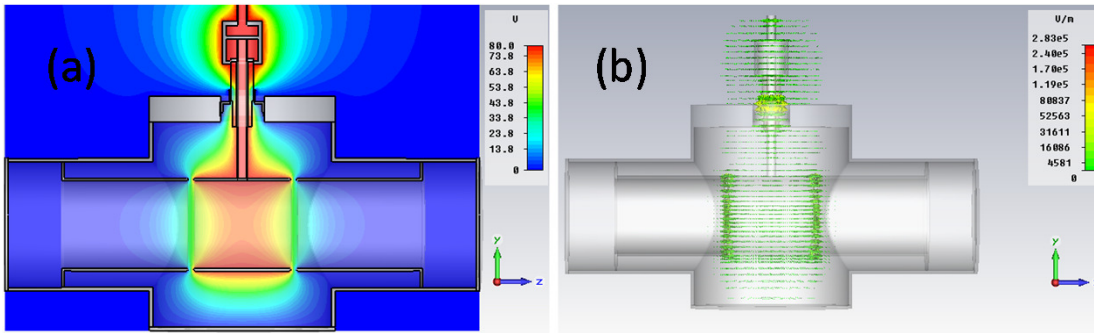
direct connection between drift-tube and matching box.



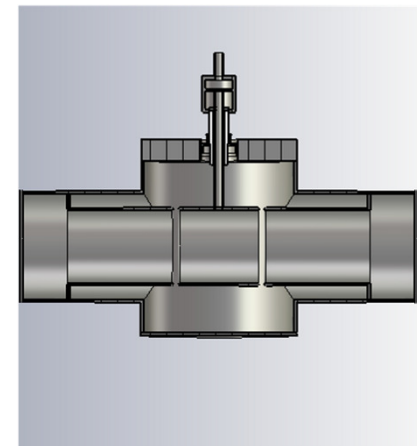
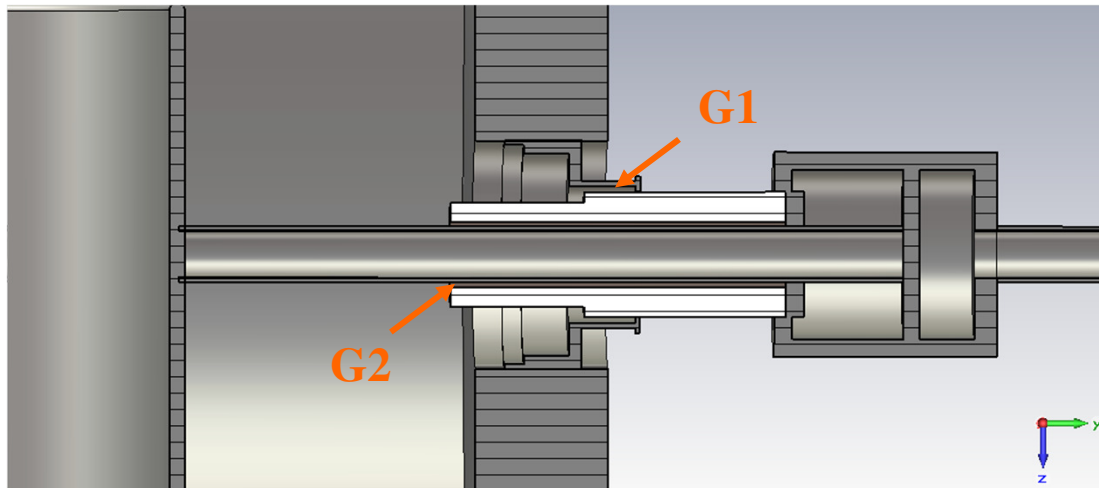
This particular design prevents any connection through coaxial transmission line. It reduces the entire geometry, the connection losses, the total RF power and the maintenance.

potential (a). 3D electric field distribution (b).

Numerical simulations



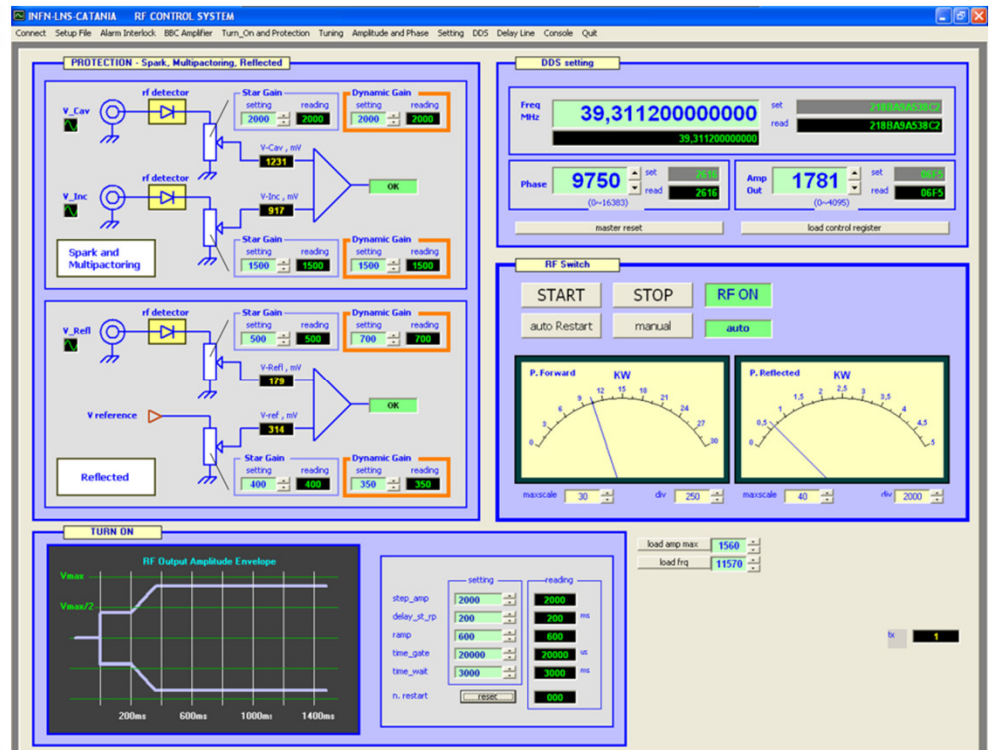
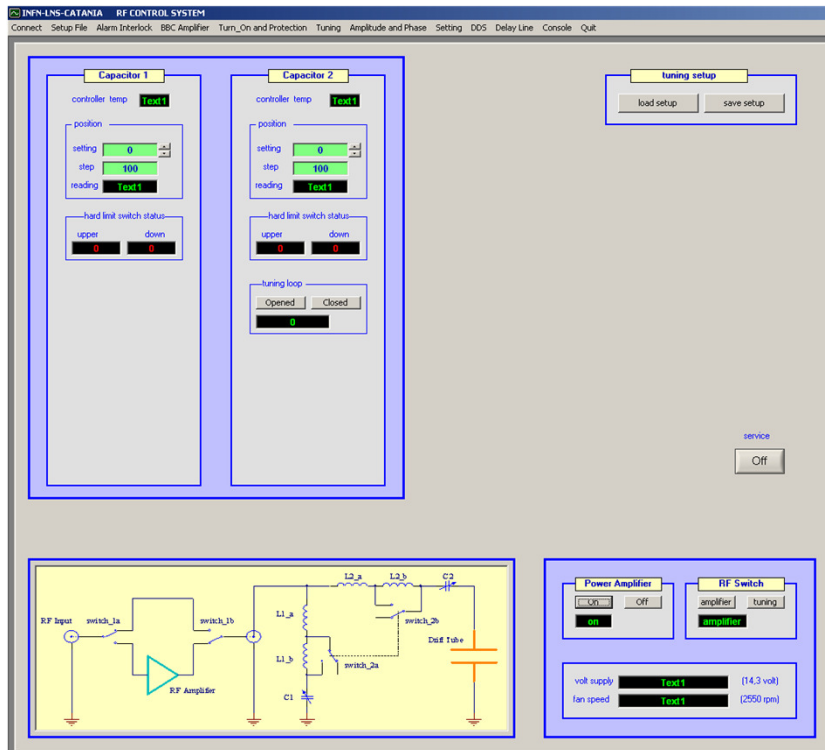
G1	G2	Mutual Capacitance	Mode 1		Mode 2		Mode 3		Mode 4	
			F	A	F	A	F	A	F	A
0.27	0.35	30.562 pF	319.3	3.034e-8	633.9	2.233e-8	869.4	3.170e-8	958.2	9.336e-8
1	0.35	29.205 pF	335.9	4.724e-8	634.8	2.348e-8	869.5	3.079e-8	958.4	1.105e-8
1	0.5	28.348 pF	352.5	5.317e-8	636.0	2.416e-8	869.5	3.031e-8	958.5	1.028e-8
1	0.8	27.778 pF	400.5	8.240e-8	640.5	4.418e-8	869.5	3.268e-8	958.9	8.600e-8
1	1.03	26.990 pF	409.0	8.407e-8	641.5	3.904e-8	869.5	2.729e-8	959.0	8.333e-8



LOW LEVEL RF

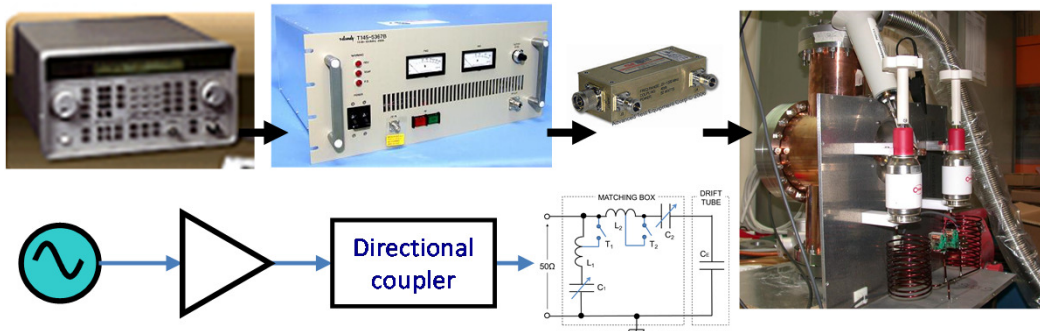
MATCHING BOX CONTROL PANEL

LLRF CONTROL PANEL SET FREQUENCY, AMPLITUDE, PHASE BY THE DDS TECHNIQUE

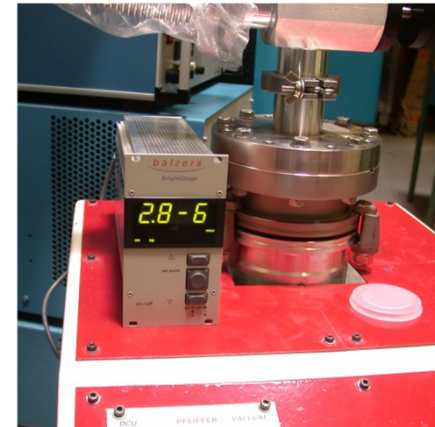


PROTECT THE SYSTEM (MULTIPACT, REFLECTED WAVE)
TURN ON/OFF THE SYSTEM (AUTO-MANUAL MODE)

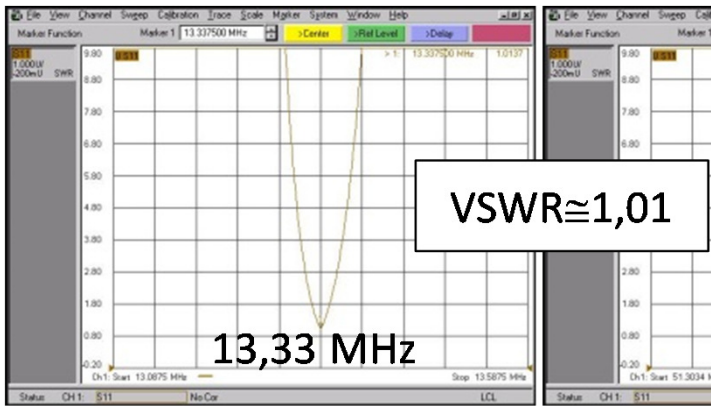
Test and measurements



BLOCK DIAGRAM



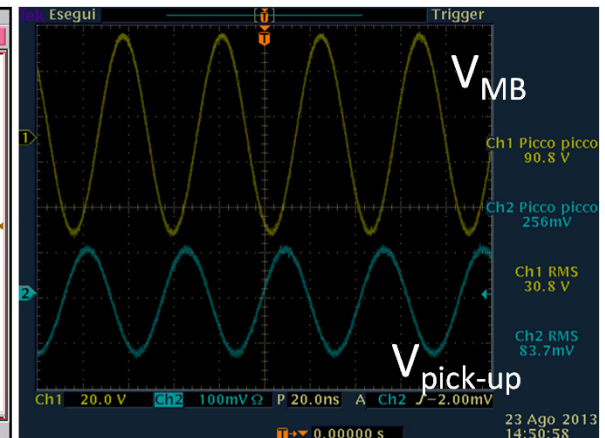
VACUUM LEVEL



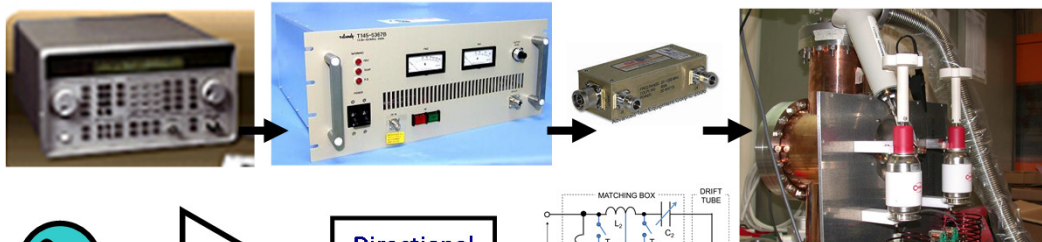
BANDWIDTH



Q-FACTOR AND VOLTAGES



Test and measurements



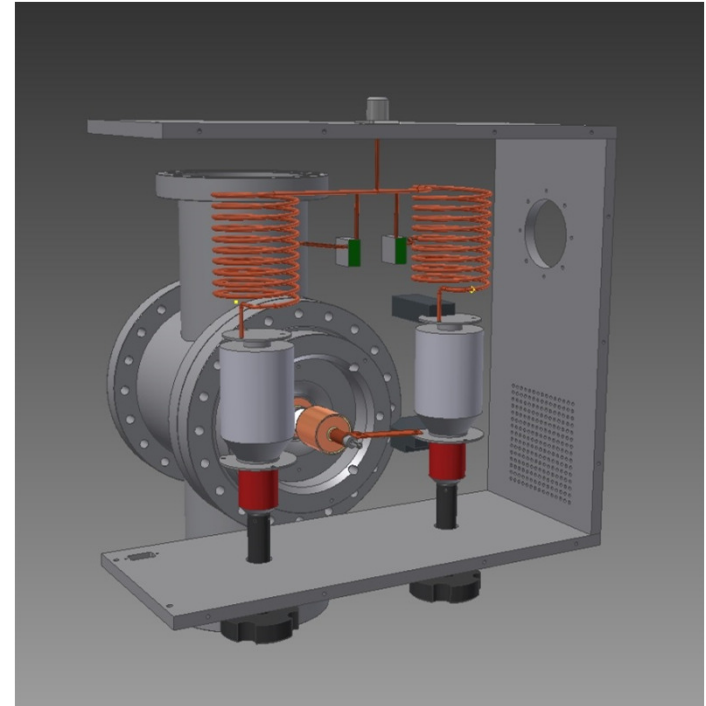
Useful mechanical/electrical tool design to measure the drift tube voltage from outside the matching box



Conclusion

Axial buncher in brief

- Frequency range 15 -50 MHz
- Voltage on the drift tube 64 -110 V
- Gain calculated about 6
- Energy spread 1,15%
- Particles transmission to the cyclotron is 57.6 %



All RF tests and measurement have been achieved at full power on the test bench. The cyclotron long maintenance programme has delayed the final test on the axial beam line of the new buncher. We believe we can produce a first test on the beam at the beginning of 2014.

Thank you for your kindly attention

References:

- D. Rifuggiato et al., "Variety of beam production at the INFN LNS Superconducting Cyclotron", MOPPT011, these proceedings.
- L. Calabretta et al, The Radiofrequency Pulsing System at INFN-LNS, USA, CYCLOTRONS 2001, p. 297.
- C. Goldstein and A. Laisne, NIM 61, 221, 1968.
- [W.J.G.M. Kleeven et al, NIM B 64, 367, 1992.
- S. Gammino et al, Review of scientific instruments volume 70, nr. 9 September 1999.
- A. Caruso et al, MOPCP057 Proceedings of CYCLOTRONS 2010, Lanzhou, China, p. 159.

A special thanks goes to:

G. Gallo, A. Longhitano INFN-LNS, Catania, Italy

J. Sura, Warsaw University, Warsaw, Poland

F. Consoli, Associazione Euratom-ENEA sulla Fusione, Frascati, Italy

Li Pengzhan, China Institute of Atomic Energy, Beijing, China